The dually localized EF-hand domain-containing protein TgEFP1 regulates the lytic cycle of *Toxoplasma gondii*

Noopur Dave, Kaice LaFavers, Gustavo Arrizabalaga*

Department of Pharmacology and Toxicology

Indiana University School of Medicine, Indianapolis, Indiana, USA.

*Address correspondence to Gustavo Arrizabalaga, garrizab@iu.edu

ABSTRACT

The propagation of the obligate intracellular parasite *Toxoplasma gondii* is tightly regulated by calcium signaling. However, the mechanisms by which calcium homeostasis and fluxes are regulated in this human pathogen are not fully understood. To identify Toxoplasma's calcium homeostasis network, we have characterized a novel EF-hand domain-containing protein, which we have named TgEFP1. We have determined that TgEFP1 localizes to a previously described compartment known as the plant-like vacuole or the endo-lysosomal compartment (PLV/ELC), which harbors several proteins related to ionic regulation. Interestingly, partial permeabilization techniques showed that TgEFP1 is also secreted into the parasitophorous vacuole (PV), within which the parasite divides. Ultrastructure expansion microscopy confirmed the unusual dual localization of TgEFP1 at the PLV/ELC and the PV. Furthermore, we determined that the localization of TgEFP1 to the PV, but not to the PLV/ELC, is affected by disruption of Golgi-dependent transport with Brefeldin A. Knockout of TgEFP1 results in faster propagation in tissue culture, hypersensitivity to calcium ionophore-induced egress, and premature natural egress. Thus, our work has revealed an interplay between the PV and the PLV/ELC and a role for TgEFP1 in the regulation of calcium-dependent events.

Keywords: *Toxoplasma*, EF-hand, calcium, egress, vacuole

1. INTRODUCTION

Calcium is a ubiquitous second messenger that regulates essential cell functions, including gene expression, protein secretion, metabolism, and apoptosis in various mammalian cell types [1]. Due to the crucial role that calcium plays in these different cellular functions, calcium levels are highly regulated, and localized calcium fluxes have been shown to regulate organelle-specific functions, including oxidative metabolism at the mitochondrial matrix and gene expression in the nucleus [1,2]. Several intracellular homeostatic mechanisms are used to regulate cytoplasmic calcium levels under resting and non-resting conditions, including activation of calcium-sensing and conducting proteins, which leads to the release or uptake of calcium by major calcium reservoirs within the cell or from the extracellular milieu [1].

Not surprisingly, calcium is also an important second messenger that regulates functions essential to the growth cycle of many eukaryotic human pathogens, including the protozoan parasite *Toxoplasma gondii* [3]. *T. gondii* infects a third of the human population and can cause severe disease in the immunocompromised and those infected congenitally [4,5]. A significant portion of this parasite's pathogenesis is due to the lytic nature of its propagation cycle. As an obligate intracellular parasite, *T. gondii* needs to be inside of a cell to divide, and it propagates by repeating cycles of host cell attachment, active invasion, and egress. Previous studies have shown that calcium plays a key role in regulating key steps of the *T. gondii* lytic cycle. Specifically, parasite-specific proteins needed for attachment and invasion are secreted in a calcium-dependent manner [3]. Furthermore, there is a temporal increase in calcium levels in the host cell, the

parasitophorous vacuole (PV) within which the parasites reside and divide, and the parasite cytosol, which regulates the timing of egress [6].

Extensive work has been conducted to understand calcium signaling in the parasite [6,7]. However, the mechanisms responsible for regulating calcium homeostasis and sensing are not thoroughly understood. The biggest calcium reservoir in mammalian cells is the endoplasmic or sarcoplasmic reticulum (ER/SR) [2]. The uptake of calcium from the ER/SR is regulated by the sarcoendoplasmic reticulum Ca^{2+}-ATPase (SERCA) [1,2]. The release of calcium from the ER/SR is regulated by 1,4,5-triphosphate receptors (IP3R) and ryanodine receptors (RyR). Similarly, the ER of *T. gondii* has been implicated in calcium storage and calcium release. Nonetheless, while the parasite is sensitive to IP3, an IP3 receptor has not been identified [6,8].

Other intracellular calcium stores in eukaryotic cells include the mitochondria, nucleus, and secretory granules in excitatory cells [2], but to date, no evidence exists for these organelles playing a role in calcium fluxes in *T. gondii*. Extensive work from our lab and others on a unique compartment known as the plant-like vacuole or the endosome-like compartment (PLV/ELC) determined that this organellar network harbors several ion binding and/or conducting proteins, including the sodium-proton exchanger 3 (TgNHE3), aquaporin (TgAQP1) and a vacuolar-pyrophosphatase (TgVP1) [9,10]. Furthermore, a calcium-proton exchanger has been predicted to localize to the PLV/ELC, suggesting that this compartment may play a role as a calcium store in the parasite [11]. However, little is known about the function of the PLV/ELC in parasite calcium homeostasis.

Interestingly, work from our lab and others has shown that the parasitophorous vacuole (PV) within which the parasite resides may also play a key role in calcium

72 regulation [3,12]. Through a forward genetic selection for parasites resistant to the effects
73 of calcium ionophores, we identified TgGRA41, a protein secreted into the PV during
74 parasite intracellular growth. Parasites lacking TgGRA41 exhibit abnormal division,
75 calcium dysregulation, and premature egress from the host [12]. We have now identified
76 a novel EF-hand domain-containing protein, TgEFP1, which is present in the PV during
77 intracellular growth. Like TgGRA41, disruption of this protein affects the timing of egress
78 and the rate of parasite propagation. Interestingly, we show that TgEFP1 is predominantly
79 present within the PLV/ELC, suggesting an interplay between this compartment and the
80 PV. Important, this work suggests that the PV and PLV/ELC collaborate in the control of
81 the parasite propagation cycle through the regulation of ionic homeostasis.

2. MATERIALS AND METHODS

Host Cell and Parasite Maintenance

All parasite strains were continuously passed through Human Foreskin Fibroblast Cells (HFF-1; ATCC Catalog #: SCRC-1041™). Cultures were maintained Dulbecco's Modified Eagle's Medium (Thermo Fischer Scientific Catalog #:11885084) supplemented with 10% heat-inactivated Fetal Bovine Serum (FBS; Corning® Catalog # 35-015-CV), 100 mg streptomycin/100 U penicillin per mL, and 2 mM L-glutamine. Cultures were grown in a humidified incubator at 37°C and 5% CO_2. The parental strain used is the RH strain lacking genes encoding hypoxanthine-xanthine-guanine phosphoribosyltransferase (*HXGPRT*) and *Ku80* (RHΔ*ku80*Δ*hxgprt*) [13,14]. Parasite lines under pyrimethamine selection were cultured in DMEM supplemented with dialyzed FBS (Corning® Catalog # 35-071-CV. Parasites were selected with pyrimethamine (1mM), mycophenolic acid (50 mg/mL) and/or xanthine (50 mg/mL). Stock pyrimethamine and mycophenolic acid were prepared in ethanol, while xanthine was prepared in water. All drugs were purchased from Sigma-Aldrich.

Generation of transgenic parasite lines

To generate the TgEFP1-HA parasite strain, a double homologous recombination strategy was used to add a triple hemagglutinin (HA) epitope tag to the endogenous gene. A fragment of homology upstream of the TgGT1_255660 stop codon was cloned into the PacI site of the pLIC-3xHA-DHFR vector by ligase-independent cloning. All primers used in this study are listed in supplemental Table S1. The resulting vector was linearized with SacI restriction enzyme and transfected into RHΔ*ku80*Δ*hxgprt* parasites. Transfected

104 parasites were selected with pyrimethamine, and clones were established by serial
105 dilution.

106 To generate the TgEFP1 knockout parasites, the TgEFP1-HA expressing strain was
107 transfected with plasmids expressing Cas9-GFP and either of two guide RNAs (sgRNA 1
108 and 2). These vectors were generated by mutating the sgRNA site in the pSag1-Cas9-
109 U6-sgUPRT-HXG plasmid [14] using the Q5 Site-Directed Mutagenesis Kit (NEB). The two
110 guide RNAs were designed to target TgEFP1 at either of the predicted EF-hand domains
111 using the online E-CRISP tool (http://www.e-crisp.org/E-CRISP/). Parasites were co-
112 transfected with either of the sgRNA expressing vectors and a donor template consisting
113 of the gene encoding HXGPRT flanked by fragments of homology to regions upstream
114 and downstream of each sgRNA. Stable lines were established through selection with
115 MPA and xanthine. Serial dilution was used to establish clones, and one from each of the
116 two populations was chosen for this work: TgEFP1-KO clone 1 from those transfected
117 with sgRNA1 and TgEFP1-KO clone 2 from the sgRNA 2 transfection. Disruption of
118 TgEFP1 in both clones was confirmed by western blot and IFA.

119 TgEFP1-KO Clone A was generated in the RHΔ*ku80*Δ*hxgprt* strain using the same
120 CRISPR/Cas9 plasmid and donor template as for TgEFP-KO clone 1. Insertion of the
121 template into the *TgEFP1* locus was confirmed by PCR. To generate a plasmid for
122 complementation, we amplified the *TgEFP1* coding sequence (CDS) from genomic DNA
123 extracted from the parental strain and a region of 1100 base pairs bases upstream of the
124 TgEFP1 start codon, which would contain the promoter and 5'UTR of the gene. Both
125 amplicons were cloned into the pLIC-3xHA-DHFR vector using In-Fusion HD Cloning to
126 obtain the plasmid 5'UTR-TgEFP1-3xHA-DHFR-HXGPRT. In-Fusion® Cloning was used

on this plasmid to generate the signal peptide deletion mutant (SP Del), in which residues 2-27 of TgEFP1 were deleted. In-Fusion® Cloning was also used to generate the D97A and D129A mutant versions of TgEFP1. The TgEFP1 WT and mutant complementation plasmids were used as templates to amplify cassettes that include efp1-EFP1-HA and the HXGPRT selection maker, which were transfected into the TgEFP1-KO Clone A strain. To direct integration of the complementation cassettes into the 5'UTR of the disrupted KU80 gene in the knockout strain, we generated plapSag1-Cas9-U6-sgKU80.5'UTR-HXGR-HXG, which expresses CAS9 and a sgRNA targeting KU80. TgEFP1-KO Clone A parasites were transfected with both the complementation cassettes and the plapSag1-Cas9-U6-sgKU80.5'UTR-HXGR-HXG plasmid. Parasites were selected with pyrimethamine, and clones were established through serial dilution. IFA was used to confirm the expression of TgEFP1 in the complemented strains.

Immunofluorescence assays and Western Blot

Immunofluorescence assays (IFAs) and western blots were performed as previously described [15-17]. For the western blots, extracellular parasite protein extract was made from parasites allowed to naturally undergo egress. Intracellular parasite extract was from HFFs infected for 30 hours. For this study, the primary antibodies used were monoclonal anti-HA rabbit and/or anti-SAG1 mouse at 1:5000, followed by goat anti-rabbit and/or goat anti-mouse conjugated to horseradish peroxidase (HRP) at 1:10,000 in non-fat dry milk in TBST (Tris buffer saline solution, 0.1% Tween 20), as previously described [15].

For immunofluorescence, assays of extracellular parasites were attached to poly-lysine treated glass coverslips as previously described [17]. For immunofluorescence assays of intracellular parasites, host cells were grown on glass coverslips and

150 subsequently infected with parasites at an MOI of 2. Samples were stained with
151 antibodies against organelle-specific primary antibodies (1:1000), including mouse anti-
152 TgATREX (apicoplast), mouse anti-TgSERCA (ER), mouse anti-F1β-ATPase
153 (mitochondrion), mouse anti-TgROP6 (rhoptries), mouse anti-TgCPL (VAC), guinea pig
154 anti-TgNHE3 (PLV), rat anti-TgSORTLR (Golgi), and mouse anti-acetylated tubulin. In
155 addition, to detect HA-tagged proteins, we used rabbit anti-HA antibodies (1:1000).
156 Secondary antibodies used were Alexa-Fluor 594 anti-Mouse (1:2000), Alexa-Fluor 748
157 anti-mouse (1:2000), Alexa-Fluor 568 anti-Guinea pig (1:2000), Alexa-Fluor 488 anti-
158 Rabbit, Alexa-Fluor 568 anti-guinea pig, and Alexa Fluor 647 anti-rat (1:2000).

159 ***Brefeldin A (BFA) Experiments***

160 Host cells were grown on 15 mm glass coverslips in 24-well plates and subsequently
161 infected with freshly lysed parasites at an MOI of 2. After 24 hours, samples were treated
162 with 0, 1, 2.5, or 5 mM BFA in HBSS for either 15 minutes, 30 minutes, or 1 hour. Samples
163 were fixed at appropriate time points in 4% paraformaldehyde/1X PBS pH 7.4 for 15
164 minutes at room temperature. IFA was performed as described above.

165 ***Ultrastructure Expansion Microscopy***

166 Host cells were seeded on 15 mm coverslips in a 24-well plate, infected with parasites
167 for 18 hours, and fixed. After fixation, ultrastructure expansion microscopy protocol was
168 used to expand and image samples as outlined in a previous study [18]. Level of
169 expansion was determined by measuring the diameter of the gel after expansion and
170 comparing it to the diameter of the coverslip. Samples were stained with the following
171 primary antibodies rabbit: anti-HA (1:500), mouse anti-TgGRA5 (1:250), and/or mouse
172 anti-acetylated tubulin. Subsequently, samples were stained with the following secondary

antibodies: goat anti-Mouse Alexa-Fluor 594, goat anti-mouse Alexa-Fluor 647, and/or goat anti-rabbit Alexa-Fluor 488. All samples were also co-stained with Alexa-Fluor 405 NHS-ester to stain for protein density.

Phenotypic assays

All phenotypic assays were performed as previously described [15,17,19]. In brief, for plaque assays, HFFs grown in 12-well plates were infected with 500 freshly lysed parasites and allowed to grow for 5-6 days, after which samples were fixed with methanol and stained with crystal violet. Imaging of samples was done using the Protein Simple FluorChem M system imager, and the plaque area clearance was quantified using ImageJ and the ColonyArea plugin [20]. For the egress assays, infected HFFs were treated with 0, 0.1, 0.5, or 1 μM of A23187 prepared in HBSS buffer (Gibco) for 2 minutes at 37°C. Samples were then fixed with methanol and stained with Hema3 Manual Staining System (Fisher Scientific). The number of intact and lysed vacuoles was recorded across all cell lines using a light microscope. For doubling assays, approximately $2x10^4$ freshly lysed parasites were allowed to invade HFFs for 2 hours, after which cultures were washed 5 times with warm media to eliminate parasites remaining outside cells. Cultures were then grown for 24 and 30 hours before fixation with methanol and staining with Hema3 Manual Staining System (Fisher Scientific). For each sample, 50 vacuoles were randomly selected, and the number of parasites per vacuole was recorded. All phenotypic assays were conducted in biological and experimental triplicate statistically analyzed using ANOVA followed by student t-tests assuming equal variance.

Statistical Analysis

All statistical analysis was performed with Microsoft Excel. All data were analyzed using Student's T-test to evaluate statistical significance.

3. RESULTS

3.1. TgEFP1-HA is localized to the PLV/ELC and the parasitophorous vacuole

To identify proteins involved in calcium regulation that might be secreted, we searched the *Toxoplasma gondii* database (ToxoDB) for proteins with both EF-hands and signal peptides. In this manner we identified TgGT1_255660, TgGT1__293760, and TgGT1_227800. User comments in ToxoDB indicate that TgGT1_293760 and TgGT1_227800 localized to the Golgi and the IMC sutures, respectively. Accordingly, we focused our investigation on the uncharacterized TgGT1_255660, a 149 amino acid protein that we refer to as TgEFP1. The online tools SignalP-5.0 and Scan Prosite predict an N-terminal signal peptide between amino acids 1 and 27 and two canonical C-terminal EF-hand domains between the amino acids 84 to 119 and 119 to 149 (Fig. 1A) [21-23]. To identify the localization and expression pattern of TgEFP1, we introduced a C-terminal triple hemagglutinin (3xHA) epitope tag along with the selectable DHFR marker at the endogenous locus using double homologous recombination (Fig. 1A). Western blot analysis probing with anti-HA primary antibody showed a specific band in the TgEFP1-HA lysate at the predicted 19 kilodaltons (kDa) size. Western blot analysis also showed that TgEFP1-HA was present in both intracellular and extracellular parasites at similar levels (Fig. 1B). Immunofluorescence assay (IFA) probing with anti-HA primary antibody showed that TgEFP1-HA localized to an internal compartment within the parasite and around the parasite cell body (Fig. 1C). IFA analysis of TgEFP1-HA parasites probing with anti-HA along with an array of organelle-specific antibodies showed that TgEFP1-HA only co-localized with the plant-like vacuole or endosomal-like compartment (PLV/ELC) marker TgNHE3 (Fig. 1D). In contrast, TgEFP1-HA did not co-localize with

other organelle markers, including TgROP6 at the rhoptries, TgCPL at the lysosome-like vacuolar compartment (VAC), TgFβ-ATPase at the mitochondrion, TgATREX at the apicoplast, and TgSERCA at the endoplasmic reticulum (Fig. 1D). Altogether, TgEFP1-HA is expressed in both intracellular and extracellular parasites and localizes to a discrete area of the parasite where it co-localizes with TgNHE3.

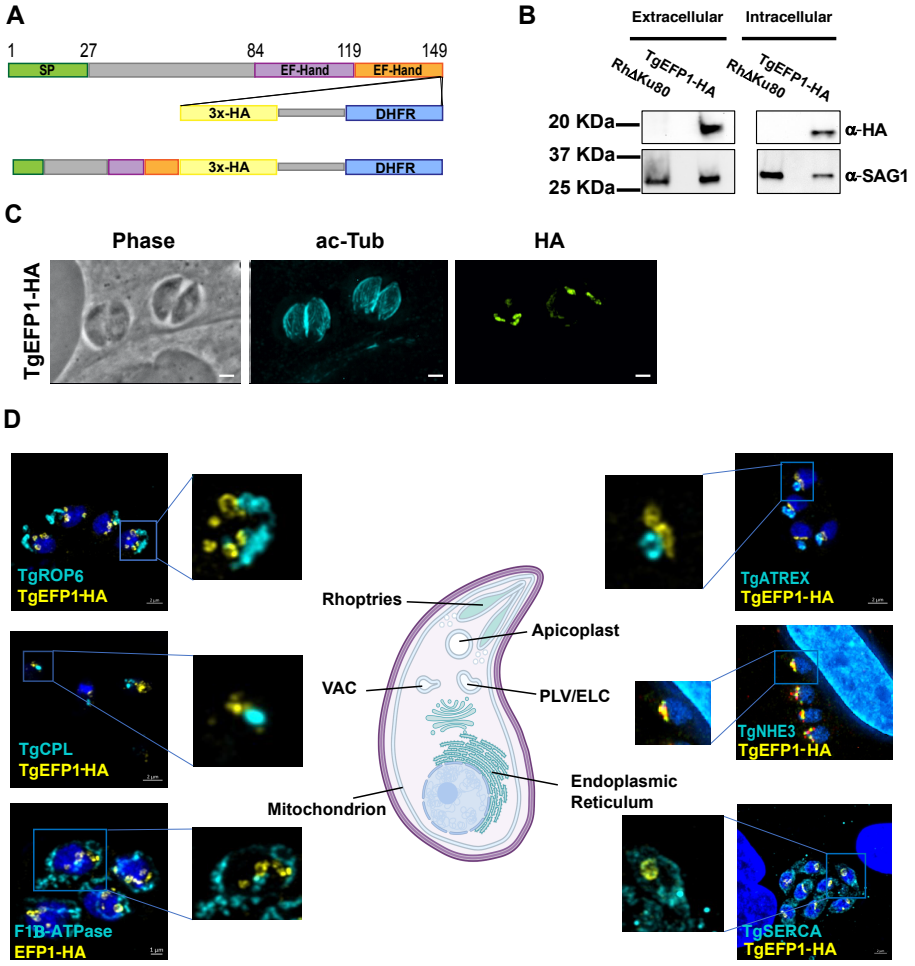

Figure 1. TgEFP1 expression and localization in intracellular and extracellular parasites. (A) Diagram of TgGT1_255660 (TgEFP1), which contains an N-terminal signal peptide (green box) along with two consecutive C-terminal EF-hand domains (purple and orange boxes). Double homologous recombination was used to introduce a triple hemagglutinin tag (3xHA, yellow box) and a DHFR selectable marker (DHFR, blue box) to the C-terminus of TgEFP1. **(B)** Western blot analysis of protein extract from both intracellular and extracellular parasites of the parental and the TgEFP1-HA strains. Blots were probed for HA (top panel) and for TgSAG1 as a loading control (bottom panel). **(C)** IFA of intracellular parasites of the TgEFP1-HA strain probing with anti-HA (green) and anti-acetylated-tubulin (cyan). **(D)** IFA of intracellular TgEFP1-HA parasites using anti-HA antibodies (green) and antibodies against known organellar markers (cyan), including ROP 6 for the rhoptries, TgCPL for the VAC, F1B-ATPase for the mitochondrion, TgATREX for the apicoplast, TgNHE3 for the PLV, and TgSERCA for the ER (Image created with BioRender.com). Scale bars = 2 mm.

Previous studies have shown that in extracellular parasites, the lysosome-like compartment named the VAC and other endosomal compartments, including the PLV/ELC, condense into one punctate region at the trans-Golgi network of the parasite [24]. The VAC then exhibits dynamic fragmentation in intracellular parasites, where it separates from the trans-Golgi network and fragments into smaller vesicles [24]. To identify if the compartment containing TgEFP1 also exhibits the same dynamic pattern, we performed IFA of intracellular and extracellular parasites probing for the trans-Golgi network marker TgSortilin-like receptor (TgSOTRTL), the known PLV/ELC marker TgNHE3, and TgEFP1-HA (Fig. 2A). in intracellular parasites the signals from all three markers appear separate from each other, where TgEFP1-HA is abutting to TgSORTLR and co-localizes with TgNHE3 (Fig. 2A, top row). However, in extracellular parasites, TgEFP1-HA co-localizes with TgSORTLR, TgNHE3, and TgEFP1-HA signals (Fig. 2A, bottom row). Thus, like other parasite endosomal compartments, the compartment harboring TgEFP1 and NHE3 exhibits dynamic events that include coalescence in extracellular parasites.

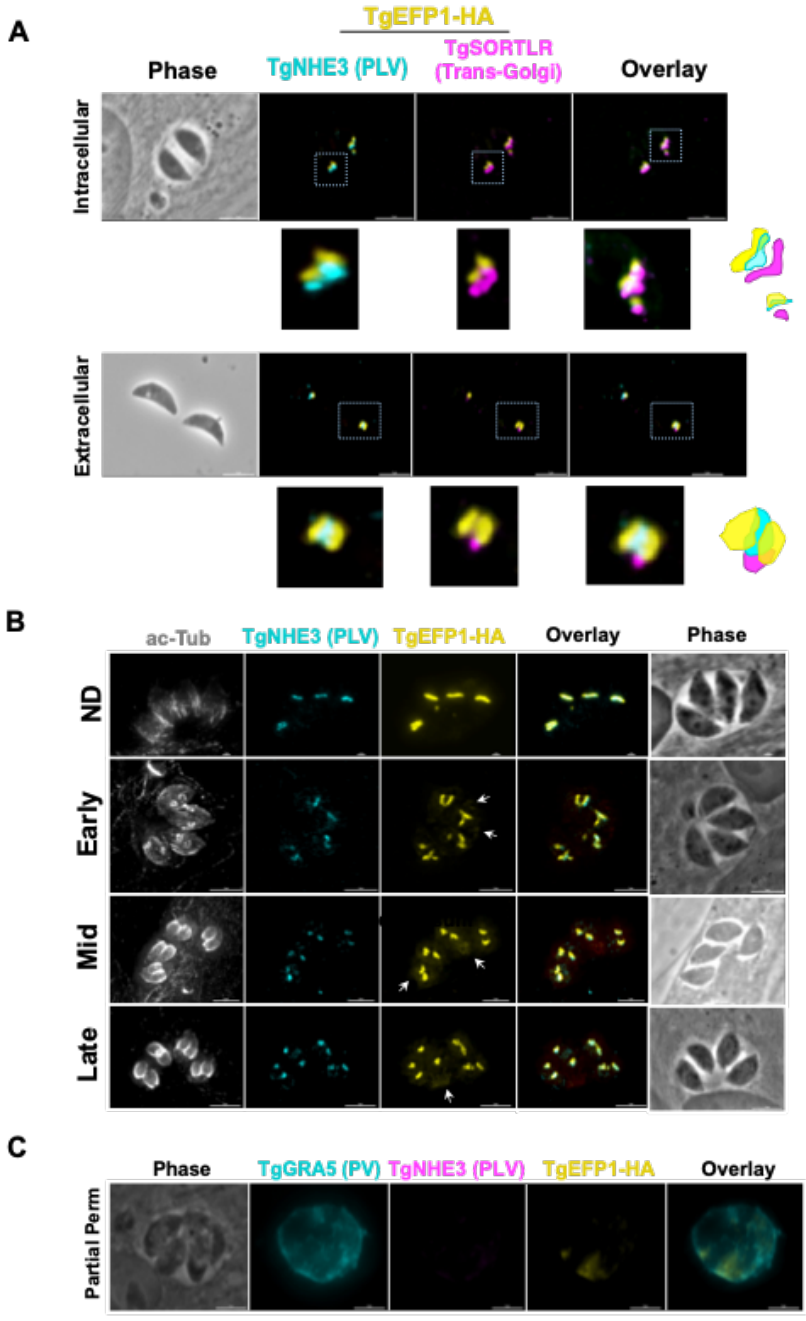

Figure 2. Dynamics of TgEFP1-HA localization during division. (A) IFA of intracellular and extracellular TgEFP1-HA parasites probed with HA antibodies (yellow), the PLV/ELC marker TgNHE3 (cyan), and the trans-Golgi marker-TgSORTLR (magenta). White box marks area zoomed on in the images below. The diagram on the right shows the relative position of the three staining patterns. **(B)** IFA of intracellular parasites using antibodies against acetylated tubulin (ac-Tub), TgNEH3, and the HA epitope tag (yellow). Acetylated tubulin was used to categorize the stage of division as either non-dividing (ND), early, mid or late. **(C)** IFA of intracellular TgEFP1-HA parasites using partial permeabilization stained for the parasitophorous vacuole (PV) marker TgGRA5 (cyan), HA (yellow), and TgNHE3. The lack of TgNHE3 staining confirms that only the host and parasitophorous vacuole membranes were permeabilized but not that of the parasite. Scale bar = 5 mm.

Closer observation of immunofluorescence images showed that the TgEFP1-HA localization pattern differed between different vacuoles. This could be due to dynamic localization during parasite division. *T. gondii* divides through a process called endodyogeny, where daughter parasites form within the mother parasite. Through this process, some organelles are inherited from the mother parasite, while other organelles are synthesized *de novo* within the daughter parasites [25]. To investigate whether the difference in TgEFP1-HA localization pattern between vacuoles was due to differences in intracellular division stages and to understand the biogenesis of its compartment, we performed IFA of intracellular parasites staining for TgEFP1 and for acetylated-tubulin, which allows us to monitor parasite division. In non-dividing parasites, TgEFP1-HA staining starts as a u-shaped pattern, one per parasite (Fig. 2B, top row). During the early division stages, the u-shaped pattern starts to distribute amongst the two daughter cells (Fig. 2B, second row). Eventually, the u-shaped pattern turns into two puncta, one per daughter parasite in mid and late division stages (Fig. 2B, third and bottom row). This showed that the variation in the TgEFP1-HA localization pattern is attributed to the dynamic pattern of its compartment during division. Furthermore, we showed that the TgEFP1-HA compartment, which appears to be the PLV/ELC, is inherited from the mother parasite.

Interestingly, during inspection of IFAs, we noted a significant amount of TgEFP1-HA signal outside of the parasites, a pattern that was more prominent in mid and late division stages (Fig. 2B, white arrow). This suggests that TgEFP1 might also be present within the parasitophorous vacuole (PV). To confirm this observation, we monitored the localization of TgEFP1 by IFA from cultures permeabilized with 0.001% digitonin, which

is known to be sufficient to permeabilize the host cell and PV membranes, but not the parasite plasma membrane [17]. Besides anti-HA antibodies to monitor TgEFP1, we stained the partially permeabilized cultures for GRA5, which is a known marker for the PV, and for TgNHE3, to confirm that the parasites remained intact. While TgNHE3 is not detectable in partially permeabilized cultures, we can clearly detect both TgGRA5 and TgEFP1 (Fig. 2C). Altogether, TgEFP1-HA has a unique dual localization at the PLV/ELC and the PV.

3.2. Monitoring of TgEFP1 localization by Ultrastructure Expansion Microscopy

As to more precisely observe the localization and dynamics of TgEFP1 in intracellular parasites, we employed Expansion Microscopy (U-ExM), which allows for higher resolution of cellular structures and protein localization [18]. Intracellular parasites were treated according to the U-ExM protocol to expand samples [18] and stained for TgEFP1-HA and TgGRA5 using antibodies and for protein density using NHS-ester. Following expansion the size of the samples increased five-fold, which revealed a high level of detail in not only the localization of TgEFP1-HA but also the dynamic fragmentation and biogenesis of the compartment within which it localizes (Fig. 3). U-ExM images show that TgEFP1-HA localizes to a discrete compartment, as seen in IFAs of non-expanded samples (Fig. 3A). Additionally, TgEFP1-HA co-localized with TgGRA5 at the PV in expanded samples, confirming the results described above (Fig. 3A). TgGRA5 is also detected within the parasite, which could be the dense granules from which this protein is secreted into the PV. Furthermore, we were able to observe TgEFP1-HA staining in the non-dividing, early, mid, and late division stages by co-staining with acetylated tubulin (Fig. 3B). In non-dividing parasites, TgEFP1-HA staining appears as puncta concentrated

309 at a focal area. During the early and mid-division stages, we see that TgEFP1-HA starts
310 to distribute amongst the two daughter parasites. Eventually, during late division stages,
311 TgEFP1-HA staining presents as two individual concentrated areas, one per daughter
312 parasite (Fig. 3B).

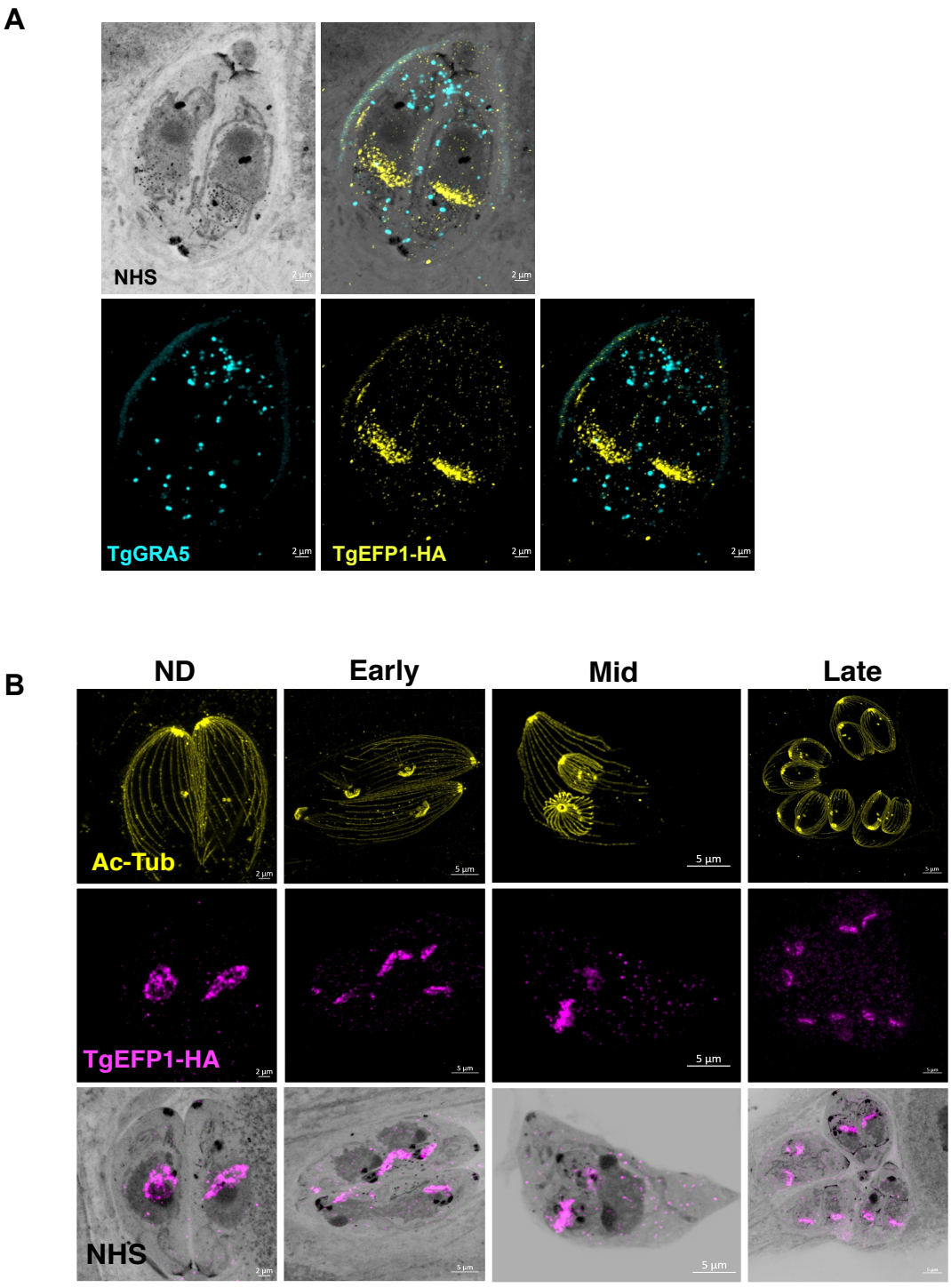

Figure 3. Ultra-structure expansion (U-ExM) microscopy of TgEFP1-HA intracellular parasites. (A) Intracellular TgEFP1-HA parasites were processed for U-ExM and stained with NHS-ester (inverted grayscale), TgGRA5 (cyan), and TgEFP1-HA (yellow). **(B)** Images show U-ExM of intracellular TgEFP1-HA parasites stained with NHS-ester (inverted grayscale), acetylated-tubulin (ac-Tub, yellow), and TgEFP1-HA (magenta). The stages of parasite division were categorized as non-dividing (ND), early, mid, and late using Ac-Tub as a guide. The bottom row shows the overlay of NHS-ester and TgEFP1-HA. Scale = 2 µm.

3.3. Brefeldin A (BFA) treatment on intracellular parasites depletes PV localization but does not affect PLV/ELC localization of TgEFP1-HA

Trafficking of secretory proteins to endosomal compartments in *T. gondii* is dependent on motor proteins and canonical vesicle transport through the Golgi complex [26]. The regulation of secretory protein trafficking through the Golgi-complex to the endosomal compartments was found to be critical for protein localization to the secretory organelles as well as for the function of those proteins [26]. To investigate the trafficking of TgEFP1-HA to the PV and its location within the parasite, intracellular parasites were treated with BFA to block ER to Golgi transport, which would inhibit the transport of proteins to endosomal compartments (Fig. 4A). IFAs of BFA treated and untreated parasites were stained with anti-HA antibodies to monitor TgEFP1-HA localization, along with acetylated-tubulin to determine the stage of intracellular division (Fig. 4B, C). Additionally, the trans-Golgi network protein TgSORTLR was used to confirm the effect of BFA, as treatment inhibits TgSORTLR trafficking to the trans-Golgi network [19]. IFA of intracellular parasites treated with 5 mM BFA for 15 minutes showed that parasites are still expressing TgSORTLR and TgEFP1-HA at intracellular compartments that are abutting each other (Fig. 4B, top row). When intracellular parasites were treated with 5 mM of BFA for 1 hour, TgSORTLR became undetectable, while the intra-parasitic foci of the TgEFP1-HA signal remained. Interestingly, we observed little to no TgEFP1-HA in the PV of vacuoles in later division stages (Fig. 4B, bottom row). In parallel, we treated parasites with 0, 1, 2.5, and 5 mM of BFA for 30 minutes. Once again, IFA of treated parasites staining with acetylated-tubulin, TgSORTLR, and TgEFP1-HA (Fig. 4C). Parasites treated with 0 and 1 mM of BFA are still expressing TgSORTLR at the trans-

Golgi network and TgEFP1-HA within the parasite with some staining at the PV (Fig. 4C, top and second row). With increasing BFA concentration to 2.5 and 5 mM, the TgSORTLR signal is diffuse or no longer present. However, TgEFP1-HA expression within the parasite remains with less to no accumulation at the PV (Fig. 4C, third and bottom row). Altogether, this showed that transport of TgEFP1-HA to the PV is Golgi-dependent, while transport of TgEFP1-HA to its intra-parasitic localization is not dependent on Golgi-transport.

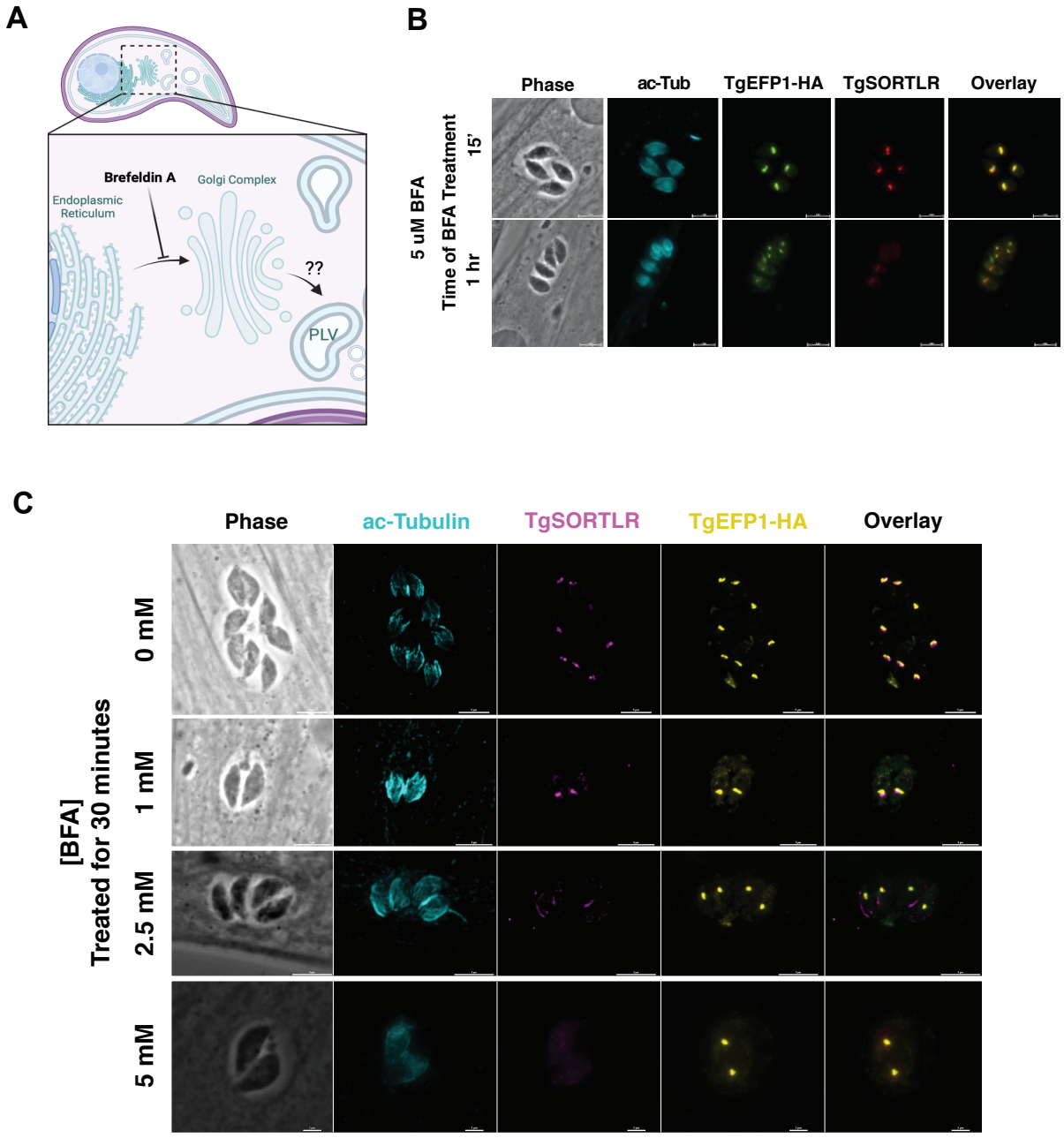

Figure 4. Effect of Brefeldin A treatment on TgEFP1-HA localization in intracellular parasites. (A) Diagram showing the effect of Brefeldin A (BFA) on protein transport and localization (created with BioRender.com). BFA inhibits vesicular fusion and transport of proteins from ER to the Golgi complex. **(B)** IFA of intracellular parasites treated with 5 mM BFA for 15 minutes (top row) or 1 hour (bottom row) stained for TgSORTLR (red), TgEFP1-HA (green), acetylated-tubulin (cyan). **(C)** IFA of intracellular parasites treated with a gradient concentration of BFA from 0 mM to 5 mM for 30 minutes and stained as in A. Scale bar = 5 μm.

3.4. TgEFP1 knockout (TgEFP1-KO) parasites have a faster lytic cycle

CRISPR/Cas9 was used to knockout TgEFP1 in the TgEFP1-HA expressing parasites to generate TgEFP1-KO parasites [13]. TgEFP1-HA parasites were co-transfected with a plasmid encoding Cas9 and one of two guide RNAs targeting TgEFP1 (sgRNA 1 and 2), along with a donor template consisting of a selectable marker flanked by regions of homology flanking the cut site in the *TgEFP1* locus (Fig. 5A). sgRNA 1 targeted the first EF-hand domain, while sgRNA 2 targeted the second EF-hand domain (Fig. 5A). In this manner, we established two independent mutant clones, where clone 1 was generated using sgRNA 1 while clone 2 was generated using sgRNA 2. Western blot of protein extracts from these clones showed that they no longer express TgEFP1-HA (Figure 5A). Protein lysate of TgEFP1-HA and parental RHΔKu80 parasites acted as positive and negative controls, respectively. IFA shows that the tagged cell lines TgEFP1 KO clones 1 and 2 are no longer expressing TgEFP1-HA but are still expressing TgNHE3 in the correct localization (Fig. 5B).

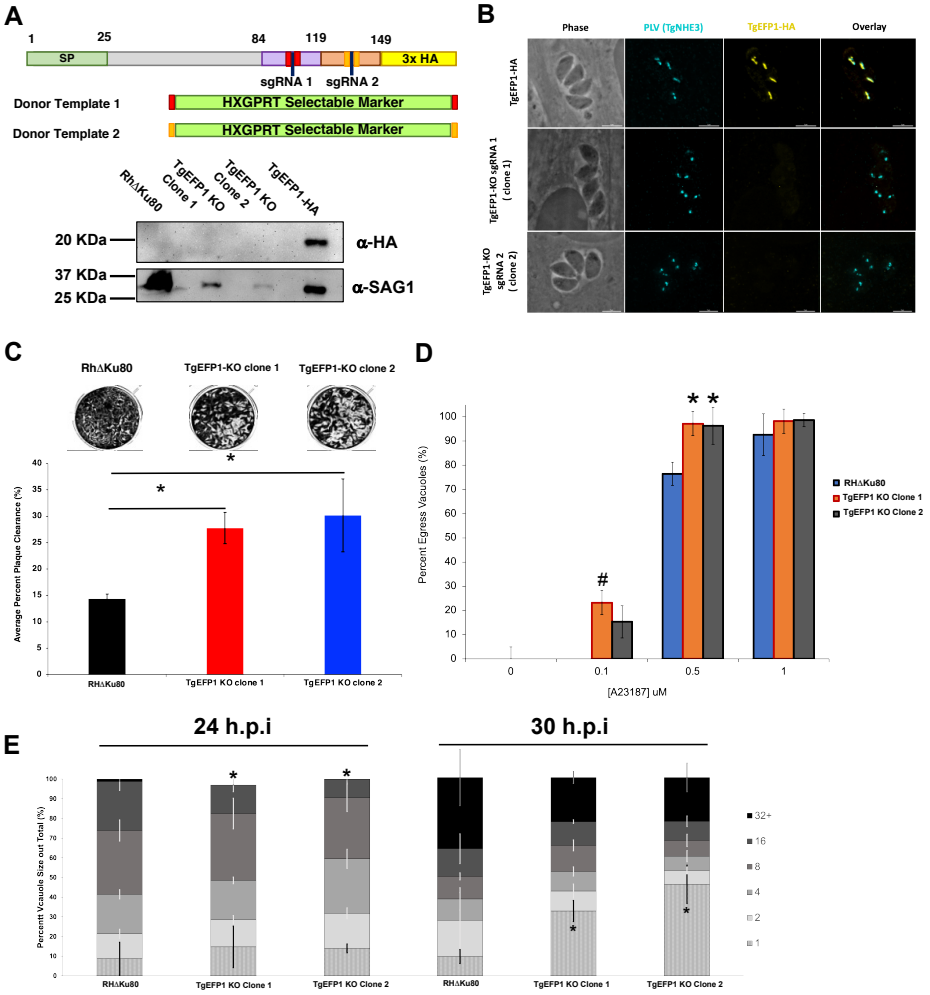

Figure 5. Generation and phenotypic analysis of TgEFP1 knockout (TgEFP1-KO) parasites. (A) Diagram showing the CRISPR/Cas9 strategy used to knockout (ko) TgEFP1 in the TgEFP1-HA strain. Two guide-RNAs (sgRNA 1 and sgRNA 2) were designed to target each of the EF-hand domains of TgEFP1. Two donor templates (1 and 2) were designed to contain the HXGPRT selectable marker flanked by regions of homology to the targeted area (red and orange boxes). The vector coding Cas9 and sgRNA1 and the donor template 1 were co-transfected to generate TgEFP1 Clone 1 and sgRNA2, and the donor template 2 were co-transfected to generate TgEFP1 Clone 2. Below the diagram is a western blot of protein extract from the parental RHΔKu80 strain, the two independent TgEFP1-KO clones, and the TgEFP1-HA parasites probed for either HA or SAG1 (loading control). **(B)** IFA of intracellular parasites of the TgEFP1-HA, TgEFP1-KO clone 1, and TgEFP1-KO clone 2 strains probed for HA (yellow) and TgNHE3 (cyan). Scale bar = 5 μm. **(C)** Representative images of plaque assays of RHΔKu80 and KO clones 1 and 2 grown for 5 days post-infection. The graph shows the quantification of plaque area clearance. **(D)** Intracellular parasites of the three strains were treated with 0, 0.1, 0.5, or 1 μM of calcium ionophore-A23187 for 2 minutes, and the percent of lysed vacuoles was calculated for each data point. **(E)** Doubling assays show that at 24 hours, there was a significantly lower number of 16 packs in comparison to parental and tagged parasites. At 30 hours, TgEFP1-KO clones 1 and 2 had a significantly higher number of 1 pack in comparison to that of parental and tagged parasites. For C to E n is 3 experimental replicates with experimental triplicates each, error bars are standard deviation; *p<0.05 and #p<0.01 based on Student's t-test.

While maintaining the parental and mutant strains, we observed that TgEFP1-KO clones 1 and 2 seemed to lyse through a monolayer of HFFs earlier than the parental parasites. To quantitate this effect, we performed plaque assays using the parental strain and the two TgEFP1-KO clones. For all phenotypic assays, we used RhΔ*hxgprt* as the parental control as there was no statistical difference between this strain and the TgEFP1-HA line. Representative images of the plaque assays show that TgEFP1-KO clones 1 and 2 have more clearance of the HFF monolayer than the parental parasites (Fig. 5C). Quantification of plaque area clearance using Image J software showed that the average percentage plaque area clearance for parental parasites was 14.395% ± 0.875, while that of TgEFP1-KO clones 1 and 2 was significantly higher at 27.79% ± 2.98 and 30.18% ± 6.87, respectively (Fig. 5C).

3.5. Parasites lacking TgEFP1 are more sensitive to ionophore induced egress

The increase in cell clearance by the KO strains could indicate a rise in the efficiency or timing of any of the steps of the parasite lytic cycle. Previous studies have shown that calcium fluxes are critical for the regulation of these steps, including the timing of parasite egress during the lytic cycle [6]. As TgEFP1 is predicted to bind calcium via two C-terminal EF-hand domains, we investigated whether the observed faster lytic rate was due to perturbations in calcium-dependent events such as egress. For this purpose, intracellular parasites were treated with 0, 0.1, 0.5, or 1 μM of the calcium ionophore A23187 for 2 minutes. For each treatment, we calculated the percentage of egressed vacuoles with respect to the no ionophore controls (Fig. 5D). At 0.1 mM of A23817 the parental strain did not exhibit any egress (0% ± 0), while TgEFP1-KO clones 1 and 2 showed 23.262% ± 11.26 and 15.37% ± 6.64 egressed vacuoles, respectively. When

parasites were treated with 0.5 mM, the trend continued where parental parasites, for which 76.44% ± 4.84 of vacuoles were ruptured, were undergoing less egress than KO clones 1 and 2, which showed 97.21% ± 7.801 and 96.32% ± 7.610 egress, respectively (Fig. 5D). This result shows that parasites lacking TgEFP1 are more sensitive to calcium ionophore treatment in comparison to the parental parasites.

Previously, we have shown that mutants that exhibit increased sensitivity to calcium ionophore-induced egress also show altered dynamics in natural egress, which could be observed by monitoring the sizes of vacuoles along time [12]. For this purpose, we tabulated the percentage of vacuoles of a particular size (i.e., number of parasites per vacuole) at 24 and 30 hours post-infection for the parental and KO strains. At 24 hours, TgEFP1 KO clones 1 and 2 had a significantly lower percentage of vacuoles with 16 parasites (14.51% ± 3.40 and 9.35% ± 1.83, respectively) in comparison to the parental strain (24.93% ± 4.56) (Fig. 5E). Interestingly, at 30 hours, TgEFP1-KO clones 1 and 2 had a significantly higher percentage of vacuoles with one parasite (32.71% ± 5.28 and 46.12% ± 9.62, respectively), in comparison to that of both RHDKu80 and TgEFP1-HA parasites (9.77% ± 3.50 and 18.20 ± 3.96, respectively) (Fig. 5E). An increase in the number of vacuoles with just one parasite would indicate that for the KO strains, the parasites are exiting the cell earlier and re-entering cells. Altogether, this showed that TgEFP1-KO clones 1 and 2 have a shorter intracellular division cycle in comparison to TgEFP1-HA parasites.

3.6. Mutating the signal peptide or EF-hands disrupts the localization pattern of TgEFP1

To test the role of various domains of TgEFP1 on its localization and function, we used a complementation approach in which we introduced either the wild-type or mutant versions of TgEFP1 into the TgEFP1-KO strains. Unfortunately, the way we created the KO strains used up the best selectable markers available and made complementation challenging. Accordingly, we created a new KO in the RHΔKu80 strain using the same CRISPR/Cas9 strategies and constructs as before. PCR analysis of TgEFP1-KO clone A showed correct insertion of the HXGPRT selectable marker at the endogenous *TgEFP1* locus (Fig. 6A). Complemented strains of the TgEFP1-KO Clone A were generated by introducing an ectopic copy of TgEFP1-HA under its endogenous promoter along with a DHFR selectable marker at the *Ku80* locus. Complementation was done with either wild-type (TgEFP1 WT), signal peptide truncation (TgEFP1 SP Del), or mutant copies containing point mutations from an aspartate residue at position 97 (TgEFP1 D97A) or 129 (TgEFP1 D129A) to an alanine (Fig. 6B). The purpose of complementing with TgEFP1 SP truncation is to understand the function of the signal peptide in the localization of the protein to the PLV/ELC and/or the PV. The purpose of complementing with point mutations at key residues within the EF-hand domains is to understand if the proteins predicted ability to bind calcium influences the localization of the protein. IFA analysis showed that TgEFP1-KO clone A parasites complemented with TgEFP1 WT-HA showed a similar localization pattern as that of endogenously tagged proteins at the PLV/ELC and the PV (Fig. 6C, left column). In contrast, TgEFP1-KO clone A parasites complemented with TgEFP1 SP Del-HA showed a localization pattern that was cytosolic puncta (Fig. 6C,

456 second column). Interestingly, TgEFP1-KO clone A parasites complemented with either
457 TgEFP1 D97A-HA or TgEFP1 D129A-HA showed a localization pattern that was
458 exclusively in the PV (Figure 6C, third and right column). Acetylated tubulin staining
459 showed that all representative vacuoles are non-dividing and outlined the cell body of the
460 parasite to allow for differentiation of localization patterns that are intra-parasitic versus
461 extra-parasitic (Fig. 6C, mid and bottom row).

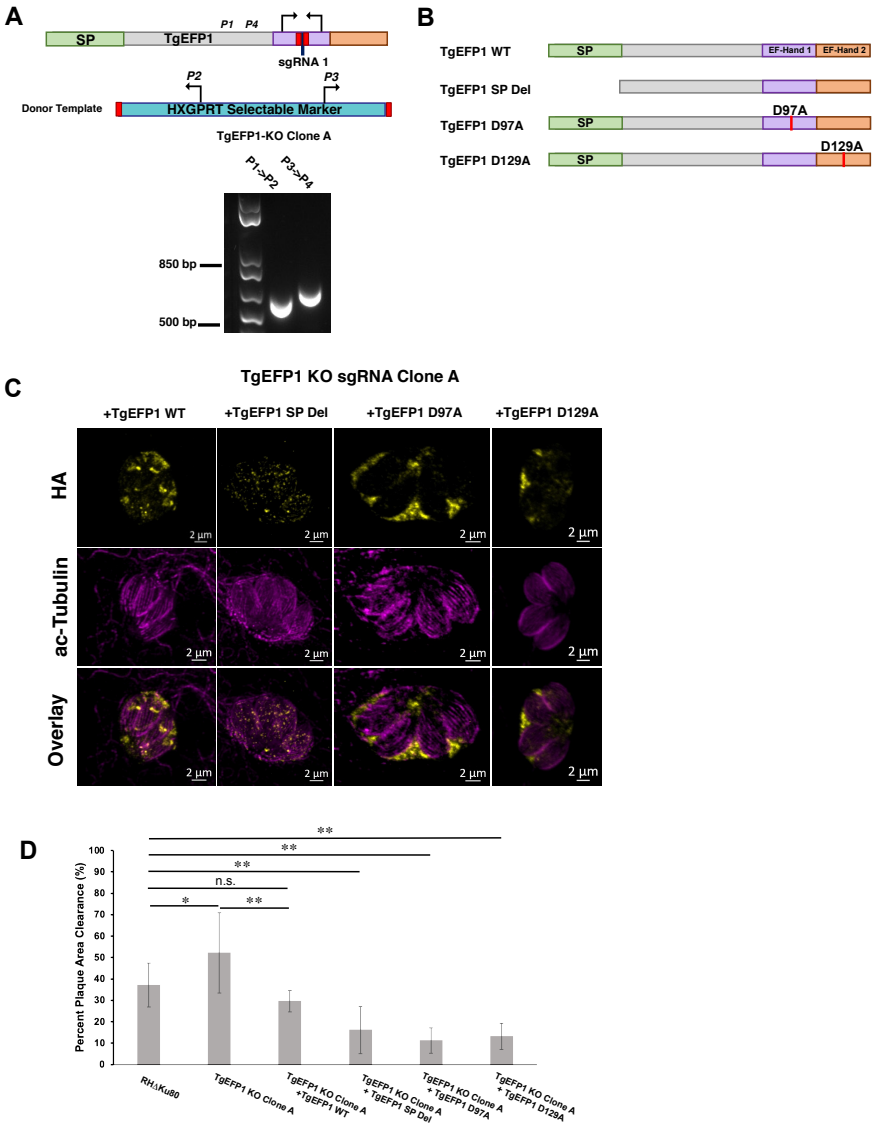

Figure 6. Role of TgEFP1 domains in localization and function. (A) Diagram of CRISPR/Cas9 strategy to generate TgEFP1-KO parasites in RHΔKu80. The sgRNA used was designed to target the first EF-hand domain (purple box). P1-4 indicates the position and direction of the primers used to confirm the integration of the donor template. Shown below diagram is the result of the PCR analysis of genomic DNA from TgEFP1-KO clone A using primer ss1 and 2 or primer 3 and 4. **(B)** Diagrams of versions of TgEFP1-HA used to complement the knockout strain. Wild-type TgEFP1-HA is shown on top. Amino acids 1 to 28 were deleted to generate the signal peptide deletion (SP Del) mutant. To disrupt the EF-hands, either the aspartic acid (D) at position 97 within EF-hand 1 or at position 129 within EF-hand 2 were mutated to alanine (A) to generate the D97A and D129A mutants. **(C)** IFA of intracellular parasites of the TgEFP1 KO Clone A strain complemented with either wild-type (+TgEFP1 WT), signal peptide deletion (+TgEFP1 SP Del), D97A (+TgEFP1 D97A), or D129A (+TgEFP1 D129A). TgEFP1 KO clone A parasites complemented TgEFP1 WT shows TgEFP1-HA (yellow) localization at the PLV and PV. TgEFP1 KO clone A parasites complemented with TgEFP1 SP Del shows TgEFP1-HA (HA; yellow) localized at intracellular puncta. TgEFP1 KO clone A parasites complemented with TgEFP1 D97A or D129A localized exclusively to the PV. All samples were co-stained with acetylated-tubulin (ac-tubulin; magenta) to ensure all representative images were of non-dividing parasites and to differentiate intra- and extracellular compartments. **(D)** Plaque assay of the parental RHΔKu80, TgEFP1 KO clone A, and all complement cell lines. Scale bar = 2 µm. *p<0.05 and **p<0.01 based on ANOVA followed by *post-hoc* Student t-tests.

Importantly, the new knockout clone TgEFP1 KO clone A showed the same plaquing phenotype as KO clones 1 and 2 (Fig. 6D). TgEFP1 KO Clone A had a significantly higher average percentage of plaque area clearance in comparison to that of the parental strain (52.10% ± 18.73 vs. 37.13% ± 10.24). This phenotype was complemented by the introduction of a wild-type copy of TgEFP1 (29.57% ± 5.00, Fig. 6D). Indeed, there was no significant difference between the plaquing efficiency of the parental strain and complemented strain (Fig. 6D). Interestingly, the three strains complemented with mutant versions of TgEFP1 propagate at a significantly lower rate than the knockout strain, which would suggest complementation of the mutant phenotype (Fig. 6D). Nonetheless, these three mutant-complemented strains are significantly less efficient at forming plaques than both the parental strain and the WT complemented strain. Thus, it is plausible that by being mislocalized and/or non-functional, these mutant versions of TgEFP1 are imparting a dominant-negative effect.

4. DISCUSSION

Calcium, one of the most pervasive second messengers, regulates vital cellular functions, including gene expression, protein secretion, metabolism, and apoptosis in a wide variety of cells [1]. For this reason, cells utilize several calcium homeostatic mechanisms to regulate calcium fluxes under resting and non-resting conditions [1]. These mechanisms include activation of calcium-sensing and/or conducting proteins, which leads to release or uptake of calcium by major calcium reservoirs within the cell or from the extracellular environment [1]. Furthermore, calcium-binding proteins can act as buffers to regulate the duration of calcium fluxes.

Out of all the calcium-binding proteins, EF-hand domain-containing ones are the most abundant [27]. The structural composition of EF-hand domains consists of a Ca^{2+}-coordinating loop that is flanked by two alpha-helices [1,28]. Specifically, the Ca^{2+}-coordinating loop comprises 5-7 ligands, which are primarily carboxylate groups arranged in a pentagonal bipyramid [28]. Most frequently, two EF-hand domains are paired to form the functional calcium-binding unit [29]. EF-hand domains are categorized as either canonical or pseudo domains [29]. Canonical EF-hand domains consist of pairs of EF-hand motifs that work in concert to coordinate calcium-binding through carboxylate groups of the residues that comprise them. In contrast, pseudo-EF-hand domains consist of a single and/or an odd number of EF-hand motifs that bind calcium through backbone carbonyl groups [28]. Due to the difference in structures between these two classes of EF-hand domains, there is a difference in calcium-binding affinities [1,29]. Specifically, canonical EF-hand domains have a relatively higher calcium-binding affinity than that of pseudo-EF-hand domains [1,29]. This leads to two main functional classes of EF-hand

516 domain-containing proteins: calcium-sensing, which are mostly comprised of pseudo-EF-
517 hand domains, and calcium buffering proteins, which are mostly comprised of canonical
518 EF-hand domains [1,29]. Furthermore, calcium buffering EF-hand domain-containing
519 proteins exhibit limited conformational changes upon calcium binding, whereas calcium-
520 sensing EF-hand domain-containing proteins exhibit large conformational changes upon
521 calcium binding to allow for interacting proteins to bind [29]. For these reasons, calcium
522 buffering EF-hand domain-containing proteins primarily play a role in modulating the
523 duration of calcium signaling and maintaining calcium homeostasis, while calcium-
524 sensing EF-hand domain proteins primarily respond to physiological changes in calcium
525 [1].

526 Just as in mammalian and plant cells, calcium also plays a key role in regulating
527 the growth cycle of the eukaryotic human pathogen *Toxoplasma gondii* [3]. Not
528 surprisingly, *Toxoplasma* encodes numerous proteins containing EF-hand domains.
529 Previous studies have identified 68 EF-hand domain-containing proteins within the
530 *Toxoplasma* genome, of which 8 contain transmembrane domains [30]. Among the most
531 studied EF-hand proteins in *Toxoplasma* are the calcium-dependent protein kinases
532 (CDPKs). CDPKs, which are unique to plants and some protozoan parasites and absent
533 in mammalian cells, contain a serine/threonine kinase domain and a calmodulin-like
534 domain linked by an autoinhibitory junction domain [31]. In *Toxoplasma*, CDPKs have
535 been implicated in a diversity of functions, including secretion, motility, invasion, egress,
536 and parasite division [32-34]. Other categories of EF-hand domain-containing proteins
537 characterized in *Toxoplasma* fall into the functional categories of calmodulin (CaM), CaM-
538 like, centrins, calcatrins, and calcineurin proteins [3]. Given the great diversity of functions

539 imparted by EF-hand proteins and the importance of calcium signaling in this parasite,
540 there is a need to characterize a broader range of EF-hand domain-containing proteins.

541 We have now identified and characterized TgEFP1, which, based on *in silico*
542 analysis of its primary and secondary structure, has a predicted N-terminal signal peptide
543 and two EF-hand domains located at the C-terminus of the protein (Fig. 1A). In-depth
544 analysis of the Ca^{2+} coordinating residues shows that the EF-hand domains contain 12
545 of them, including two aspartic acid residues at positions 97 and 129, suggesting that
546 TgEFP1 contains canonical EF-hand domains. For this reason, it is predicted that
547 TgEFP1 acts as a calcium buffering protein and may play a role in modulating the duration
548 of calcium fluxes and maintaining calcium homeostasis in the parasite. Furthermore, no
549 transmembrane domains and/or post-translational modification were predicted that would
550 suggest the protein was membrane-associated. Therefore, TgEFP1 would be the first
551 identified luminal protein of the PLV/ELC.

552 Interestingly, TgEFP1 can be detected both in the PLV/ELC and within the
553 parasitophorous vacuole (PV). To our knowledge, this is the first report of a *Toxoplasma*
554 protein that localizes to both the PLV/ELC and the PV, suggesting a crosstalk between
555 these two organelles. Previous studies have identified crosstalk between the endocytic
556 and exocytic system, where the VAC played a key role in the export and import of proteins
557 from the PV and host cell to the parasite cell body [35]. Since the VAC and other
558 compartments of the endo-lysosomal system, including the PLV/ECL, can fuse in
559 extracellular parasites. It is possible that there is an exchange of contents between all of
560 these compartments. Thus, the dual localization of TgEFP1 may be attributed to
561 interactions between *Toxoplasma's* endocytic and exocytic systems.

Lack of TgEFP1 results in disruption of the normal propagation of the parasite as well as an altered sensitivity to calcium ionophores. These phenotypes would suggest that TgEFP1 plays a role in calcium-dependent processes and/or homeostasis. As TgEFP1 is in both the PV and the PLV/ELC, a question arises as to in which of those two locations is TgEFP1's function being imparted. Interestingly, the phenotypic defects observed in the TgEFP1 knockout parasites parallel those of parasites lacking the PV localized dense granule protein GRA41 [12]. GRA41 is a dense granule protein that is secreted into the PV, and loss of GRA41 leads to defects in calcium regulation and timing of egress [12]. The fact that loss of either GRA41 or TgEFP1 results in premature egress might suggest that events at the PV might act as a hub for regulation of parasite exit and a plausible locale for TgEFP1's function.

Nonetheless, it is also plausible that TgEFP1 acts within the PLV/ELC. Lysosomes, endosomal vesicles, peroxisomes, and secretory vesicles can function in calcium release to induce signaling that regulates localized cellular functions, including protein transport, protein secretion, and vesicle fusion [36]. Unique to plant cells are EF-hand domain proteins that localize to the plant vacuole [37,38]. The EF-hand domain proteins that are specific to plant vacuoles play a key role in mediating calcium signaling that is implicated in osmoregulation under stress conditions, including drought, cold, and salt stress [37]. Furthermore, plant EF-hand domain-containing proteins regulate calcium signaling, which is vital to plant adaptive behavior [37]. Lastly, the plant vacuole has been shown to be a major calcium reservoir within plant cells, where the entry and release of calcium are regulated by the EF-hand domain-containing proteins that localize to the plant vacuole [37,38]. Therefore, the PLV/VAC may also play a role as a calcium reservoir in the parasite,

585 and TgEFP1 may play an important in adaptive behaviors and osmoregulation in the
586 parasite.

587 To start addressing the relation between function and localization for TgEFP1, we
588 investigated the consequence of mutating the signal peptide. Unfortunately, this mutant
589 protein was not localized to either the PLV or the PV and appeared to cause a dominant
590 negative effect. Interestingly, when we mutated either of the EF-hand domains, TgEFP1
591 was only present in the PV. This suggests that the binding of calcium by both EF-hand
592 domains is necessary for the localization of the protein to the PLV/ELC. Therefore, we
593 speculate that TgEFP1 is initially secreted to the PV, and upon binding to calcium, it is
594 internalized to the PLV/ELC as a mechanism to regulate calcium homeostasis within the
595 parasite. This model is consistent with our observations that TgEFP1-HA transport to the
596 PV is Golgi-dependent, while transport to the PLV/ELC is not. Furthermore, the endocytic
597 and exocytic systems of the parasite are known to converge at endosomal compartments
598 to regulate the import and export of proteins from the parasite cell body [35]. Thus, through
599 the function of TgEFP1, the PV and the endosomal compartments might be collaborating
600 in regulating calcium homeostasis and facilitating calcium signaling.

601 In terms of function, TgEFP1 may act as a calcium buffer that actively regulates
602 levels of calcium within the PV, parasite cytosol, and the PLV/ELC. Specifically, TgEFP1
603 may initially be transported to the PV, where it binds to excess calcium. Upon binding to
604 calcium, the protein is internalized through the function of the PLV/ELC. The calcium is
605 then retained in the PLV/ELC to also regulate calcium levels within the parasite cytosol.
606 Future directions will be to identify and characterize TgEFP1 interactors that also localize
607 to the PLV/ELC to gain a better understanding of its function in the parasite. Lastly,

608 calcium studies, including the use of live calcium indicators, could determine the
609 functional relevance of TgEFP1 indirectly regulating calcium fluxes within the parasite
610 cytosol and the PV during the lytic cycle of the parasite.

ACKNOWLEDGMENTS

We would like to thank Dr. Sabrina Absalon and Dr. Benjamin Liffner for their assistance with the expansion microscopy experiments. This research was supported by the National Institute of Health grants R01AI123457, R01AI149766, RO1AI89808, and R21AI124067 to GA. ND was funded by a pre-doctoral fellowship from the American Heart Association (834981).

REFERENCES

1. Bagur, R.; Hajnóczky, G. Intracellular Ca. *Mol Cell* **2017**, *66*, 780-788, doi:10.1016/j.molcel.2017.05.028.
2. Prins, D.; Michalak, M. Organellar calcium buffers. *Cold Spring Harb Perspect Biol* **2011**, *3*, doi:10.1101/cshperspect.a004069.
3. Hortua Triana, M.A.; Márquez-Nogueras, K.M.; Vella, S.A.; Moreno, S.N.J. Calcium signaling and the lytic cycle of the Apicomplexan parasite Toxoplasma gondii. *Biochim Biophys Acta Mol Cell Res* **2018**, *1865*, 1846-1856, doi:10.1016/j.bbamcr.2018.08.004.
4. Robert-Gangneux, F.; Dardé, M.L. Epidemiology of and diagnostic strategies for toxoplasmosis. *Clin Microbiol Rev* **2012**, *25*, 264-296, doi:10.1128/CMR.05013-11.
5. Montoya, J.G.; Rosso, F. Diagnosis and management of toxoplasmosis. *Clin Perinatol* **2005**, *32*, 705-726, doi:10.1016/j.clp.2005.04.011.
6. Borges-Pereira, L.; Budu, A.; McKnight, C.A.; Moore, C.A.; Vella, S.A.; Hortua Triana, M.A.; Liu, J.; Garcia, C.R.; Pace, D.A.; Moreno, S.N. Calcium Signaling throughout the Toxoplasma gondii Lytic Cycle: A STUDY USING GENETICALLY ENCODED CALCIUM INDICATORS. *J Biol Chem* **2015**, *290*, 26914-26926, doi:10.1074/jbc.M115.652511.
7. Pace, D.A.; McKnight, C.A.; Liu, J.; Jimenez, V.; Moreno, S.N. Calcium entry in Toxoplasma gondii and its enhancing effect of invasion-linked traits. *J Biol Chem* **2014**, *289*, 19637-19647, doi:10.1074/jbc.M114.565390.
8. Smith, J.E. A ubiquitous intracellular parasite: the cellular biology of Toxoplasma gondii. *Int J Parasitol* **1995**, *25*, 1301-1309, doi:10.1016/0020-7519(95)00067-c.
9. Francia, M.E.; Wicher, S.; Pace, D.A.; Sullivan, J.; Moreno, S.N.; Arrizabalaga, G. A Toxoplasma gondii protein with homology to intracellular type Na^+/H^+ exchangers is important for osmoregulation and invasion. *Exp Cell Res* **2011**, *317*, 1382-1396, doi:10.1016/j.yexcr.2011.03.020.
10. Liu, J.; Pace, D.; Dou, Z.; King, T.P.; Guidot, D.; Li, Z.H.; Carruthers, V.B.; Moreno, S.N. A vacuolar-H(+) -pyrophosphatase (TgVP1) is required for microneme secretion, host cell invasion, and extracellular survival of Toxoplasma gondii. *Mol Microbiol* **2014**, *93*, 698-712, doi:10.1111/mmi.12685.
11. Miranda, K.; Pace, D.A.; Cintron, R.; Rodrigues, J.C.; Fang, J.; Smith, A.; Rohloff, P.; Coelho, E.; de Haas, F.; de Souza, W.; et al. Characterization of a novel organelle in Toxoplasma gondii with similar composition and function to the plant vacuole. *Mol Microbiol* **2010**, *76*, 1358-1375, doi:10.1111/j.1365-2958.2010.07165.x.
12. LaFavers, K.A.; Márquez-Nogueras, K.M.; Coppens, I.; Moreno, S.N.J.; Arrizabalaga, G. A novel dense granule protein, GRA41, regulates timing of egress and calcium sensitivity in Toxoplasma gondii. *Cell Microbiol* **2017**, *19*, doi:10.1111/cmi.12749.
13. Shen, B.; Brown, K.; Long, S.; Sibley, L.D. Development of CRISPR/Cas9 for Efficient Genome Editing in Toxoplasma gondii. *Methods Mol Biol* **2017**, *1498*, 79-103, doi:10.1007/978-1-4939-6472-7_6.
14. Long, S.; Brown, K.M.; Sibley, L.D. CRISPR-mediated Tagging with BirA Allows Proximity Labeling in. *Bio Protoc* **2018**, *8*, doi:10.21769/BioProtoc.2768.

15. Yang, C.; Broncel, M.; Dominicus, C.; Sampson, E.; Blakely, W.J.; Treeck, M.; Arrizabalaga, G. A plasma membrane localized protein phosphatase in Toxoplasma gondii, PPM5C, regulates attachment to host cells. *Sci Rep* **2019**, *9*, 5924, doi:10.1038/s41598-019-42441-1.
16. Blakely, W.J.; Holmes, M.J.; Arrizabalaga, G. The Secreted Acid Phosphatase Domain-Containing GRA44 from Toxoplasma gondii Is Required for c-Myc Induction in Infected Cells. *mSphere* **2020**, *5*, doi:10.1128/mSphere.00877-19.
17. Jacobs, K.; Charvat, R.; Arrizabalaga, G. Identification of Fis1 Interactors in Toxoplasma gondii Reveals a Novel Protein Required for Peripheral Distribution of the Mitochondrion. *mBio* **2020**, *11*, doi:10.1128/mBio.02732-19.
18. Liffner, B.; Absalon, S. Expansion Microscopy Reveals. *Microorganisms* **2021**, *9*, doi:10.3390/microorganisms9112306.
19. Heredero-Bermejo, I.; Varberg, J.M.; Charvat, R.; Jacobs, K.; Garbuz, T.; Sullivan, W.J.; Arrizabalaga, G. TgDrpC, an atypical dynamin-related protein in Toxoplasma gondii, is associated with vesicular transport factors and parasite division. *Mol Microbiol* **2019**, *111*, 46-64, doi:10.1111/mmi.14138.
20. Guzman, C.; Bagga, M.; Kaur, A.; Westermarck, J.; Abankwa, D. ColonyArea: an ImageJ plugin to automatically quantify colony formation in clonogenic assays. *PLOS ONE* **2014**, *9*, e92444, doi:10.1371/journal.pone.0092444.
21. Vakili, O.; Khatami, S.H.; Maleksabet, A.; Movahedpour, A.; Fana, S.E.; Sadegh, R.; Salmanzadeh, A.H.; Razeghifam, H.; Nourdideh, S.; Tehrani, S.S.; et al. Finding Appropriate Signal Peptides for Secretory Production of Recombinant Glucarpidase: An In SilicoMethod. *Recent Pat Biotechnol* **2021**, *15*, 302-315, doi:10.2174/1872208315666210921095420.
22. de Castro, E.; Sigrist, C.J.; Gattiker, A.; Bulliard, V.; Langendijk-Genevaux, P.S.; Gasteiger, E.; Bairoch, A.; Hulo, N. ScanProsite: detection of PROSITE signature matches and ProRule-associated functional and structural residues in proteins. *Nucleic Acids Res* **2006**, *34*, W362-365, doi:10.1093/nar/gkl124.
23. Sigrist, C.J.; Cerutti, L.; Hulo, N.; Gattiker, A.; Falquet, L.; Pagni, M.; Bairoch, A.; Bucher, P. PROSITE: a documented database using patterns and profiles as motif descriptors. *Brief Bioinform* **2002**, *3*, 265-274, doi:10.1093/bib/3.3.265.
24. Huang, R.; Que, X.; Hirata, K.; Brinen, L.S.; Lee, J.H.; Hansell, E.; Engel, J.; Sajid, M.; Reed, S. The cathepsin L of Toxoplasma gondii (TgCPL) and its endogenous macromolecular inhibitor, toxostatin. *Mol Biochem Parasitol* **2009**, *164*, 86-94.
25. Nishi, M.; Hu, K.; Murray, J.M.; Roos, D.S. Organellar dynamics during the cell cycle of Toxoplasma gondii. *J Cell Sci* **2008**, *121*, 1559-1568, doi:10.1242/jcs.021089.
26. Carmeille, R.; Schiano Lomoriello, P.; Devarakonda, P.M.; Kellermeier, J.A.; Heaslip, A.T. Actin and an unconventional myosin motor, TgMyoF, control the organization and dynamics of the endomembrane network in Toxoplasma gondii. *PLoS Pathog* **2021**, *17*, e1008787, doi:10.1371/journal.ppat.1008787.
27. Halling, D.B.; Liebeskind, B.J.; Hall, A.W.; Aldrich, R.W. Conserved properties of individual Ca2+-binding sites in calmodulin. *Proc Natl Acad Sci U S A* **2016**, *113*, E1216-1225, doi:10.1073/pnas.1600385113.

28. Strynadka, N.C.; James, M.N. Crystal structures of the helix-loop-helix calcium-binding proteins. *Annu Rev Biochem* **1989**, *58*, 951-998, doi:10.1146/annurev.bi.58.070189.004511.
29. Schwaller, B. Cytosolic Ca2+ buffers. *Cold Spring Harb Perspect Biol* **2010**, *2*, a004051, doi:10.1101/cshperspect.a004051.
30. Chang, L.; Dykes, E.J.; Li, J.; Moreno, S.N.J.; Hortua Triana, M.A. Characterization of Two EF-hand Domain-containing Proteins from Toxoplasma gondii. *J Eukaryot Microbiol* **2019**, *66*, 343-353, doi:10.1111/jeu.12675.
31. Asai, S.; Ichikawa, T.; Nomura, H.; Kobayashi, M.; Kamiyoshihara, Y.; Mori, H.; Kadota, Y.; Zipfel, C.; Jones, J.D.G.; Yoshioka, H. The variable domain of a plant calcium-dependent protein kinase (CDPK) confers subcellular localization and substrate recognition for NADPH oxidase. *J Biol Chem* **2013**, *288*, 14332-14340, doi:10.1074/jbc.M112.448910.
32. Cardew, E.M.; Verlinde, C.L.M.J.; Pohl, E. The calcium-dependent protein kinase 1 from Toxoplasma gondii as target for structure-based drug design. *Parasitology* **2018**, *145*, 210-218, doi:10.1017/S0031182017001901.
33. Gaji, R.Y.; Johnson, D.E.; Treeck, M.; Wang, M.; Hudmon, A.; Arrizabalaga, G. Phosphorylation of a Myosin Motor by TgCDPK3 Facilitates Rapid Initiation of Motility during Toxoplasma gondii egress. *PLoS Pathog* **2015**, *11*, e1005268, doi:10.1371/journal.ppat.1005268.
34. McCoy, J.M.; Whitehead, L.; van Dooren, G.G.; Tonkin, C.J. TgCDPK3 regulates calcium-dependent egress of Toxoplasma gondii from host cells. *PLoS Pathog* **2012**, *8*, e1003066, doi:10.1371/journal.ppat.1003066.
35. McGovern, O.L.; Rivera-Cuevas, Y.; Kannan, G.; Narwold, A.J.; Carruthers, V.B. Intersection of endocytic and exocytic systems in Toxoplasma gondii. *Traffic* **2018**, *19*, 336-353, doi:10.1111/tra.12556.
36. Yang, J.; Zhao, Z.; Gu, M.; Feng, X.; Xu, H. Release and uptake mechanisms of vesicular Ca. *Protein Cell* **2019**, *10*, 8-19, doi:10.1007/s13238-018-0523-x.
37. Mohanta, T.K.; Yadav, D.; Khan, A.L.; Hashem, A.; Abd Allah, E.F.; Al-Harrasi, A. Molecular Players of EF-hand Containing Calcium Signaling Event in Plants. *Int J Mol Sci* **2019**, *20*, doi:10.3390/ijms20061476.
38. Day, I.S.; Reddy, V.S.; Shad Ali, G.; Reddy, A.S. Analysis of EF-hand-containing proteins in Arabidopsis. *Genome Biol* **2002**, *3*, RESEARCH0056, doi:10.1186/gb-2002-3-10-research0056.

SUPPLEMENTAL MATERIALS

Supplemental Table S1. Primers used in this study.

Purpose	Name	Sequence
Generate vector to tag endogenous TgEFP1	EFP1HA forward	cccccgcgcttcctgccaccaagcttcgccaggctgt
	EFP1HA reverse	accgttctcgccagtttcacCAtCctgcaaGtgcatagaaggaa
Generate pSag1-Cas9-U6-sg1EFP1 by using Q5 mutagenesis	EFP1SG1 forward	ccaacggagagttttagagctagaaatagc
	EFP1SG1 reverse	agtcgaactcaacttgacatccccatttac
Amplifying donor template for knockout clone 1	DonorKO1 forward	ggacgaagacgacgaggccttcatccgcgaggaattcatggaacaa aagttgatttctgaagaag
	DonorKO1 reverse	tgcttctttcctcctctgtgttcctgctttttgacgcctagcggaagatccgat cttgc
Generate pSag1-Cas9-U6-sg2EFP1 by using Q5 mutagenesis	EFP1SG2 forward	ttccggctaggttttagagctagaaatagc
	EFP1SG2 reverse	gaaagaaaacaacttgacatccccatttac
Amplifying donor template for knockout clone 1	DonorKO2 forward	aggtccgagtgacgcatcccgaaatcggaaacagcgaactgaacaa aagttgatttctgaagaag
	DonorKO2 reverse	cgatattctgcgagagtcaagagtccatcttggttggagtgcggaagat ccgatcttg
Amplifying TgEFP1 gDNA to make complementing construct	TgEFP1comp WT forward	ggaggacgggaattcaaggagatggggacggcg
	TgEFP1comp WT reverse	gttccctagggaattcaatagctgatgatacatactcgcgatatt
Deleting signal peptide from complementing construct	ΔSP forward	ccaccatgttcgcgcgcctggcgtcg
	ΔSP reverse	gcgcgaacatggtggcaggaagcgc
Generation of D97A complementation construct using Q5	D97A forward	catggagtacgcatccaacggag
	D97A reverse	aattcctcgcggatgaag
	D129A forward	ccggctagtggcatccaaccaag

Generation of D129A complementation construct using Q5	D129A reverse	aagaaagaaaacagttcgc
Targeting complementing template to Ku80 locus	KU80 forward	gtccccggttcgcctcagcacacacacacatgacgtacatcgaggga acaaaagctgggtac
	KU80 reverse	ggatagctccattgtttctgatgggaactattccgacattacattcatcctg caagtgcatagaaggaa

739